Fire-vegetation interactions in Arctic tundra and their spatial variability

Dong Chen (itscd@umd.edu)*[1], Cheng Fu (cheng.fu@geo.uzh.ch)[2], Liza K. Jenkins (lliverse@mtu.edu)[3], Jiaying He (hejiaying0608@gmail.com)[1,4], Randi R. Jandt (rjandt@alaska.edu)[5], Gerald V. Frost (jfrost@abrinc.com)[6], Allison Baer (aebaer@terpmail.umd.edu)[1], Tatiana V. Loboda (loboda@umd.edu)[1]

[1]Department of Geographical Sciences, University of Maryland, College Park, MD, USA

[2]Department of Geography, University of Zurich, Zurich, Switzerland

[3]Michigan Tech Research Institute, Michigan Technological University, Ann Arbor, MI, USA

[4]Department of Earth System Science, Tsinghua University, Beijing, China

[5]Alaska Fire Science Consortium, University of Alaska, Fairbanks, AK, USA

[6]Alaska Biological Research, Inc., Fairbanks, AK, USA

[*]Corresponding author.

This manuscript is a non-peer reviewed preprint submitted to EarthArXiv. This paper is in review at Nature Plants.

Fire-vegetation interactions in Arctic tundra and their spatial variability

Dong Chen (itscd@umd.edu)*[1], Cheng Fu (cheng.fu@geo.uzh.ch)[2], Liza K. Jenkins (lliverse@mtu.edu)[3], Jiaying He (hejiaying0608@gmail.com)[1,4], Randi R. Jandt (rjandt@alaska.edu)[5], Gerald V. Frost (jfrost@abrinc.com)[6], Allison Baer (aebaer@terpmail.umd.edu)[1], Tatiana V. Loboda (loboda@umd.edu)[1]

[1]Department of Geographical Sciences, University of Maryland, College Park, MD, USA

[2]Department of Geography, University of Zurich, Zurich, Switzerland

[3]Michigan Tech Research Institute, Michigan Technological University, Ann Arbor, MI, USA

[4]Department of Earth System Science, Tsinghua University, Beijing, China

[5]Alaska Fire Science Consortium, University of Alaska, Fairbanks, AK, USA

[6]Alaska Biological Research, Inc., Fairbanks, AK, USA

[*]Corresponding author.

Abstract

Circumpolar tundra has experienced a greater increase in temperatures compared to any other biome, with a magnitude of the increase nearly three times the global average. Widespread shrubification associated with pronounced observed warming is gradually transforming the tundra ecosystem structure and function. This study confirms that a shrub-dominated fire-biomass positive feedback loop is evident across the Alaskan tundra. Tundra wildfires, especially those with higher severity, play a critical role in boosting the overall “greening” ongoing in many parts of the tundra. However, the fire-vegetation interactions are highly non-uniform and vary greatly within different tundra subregions, a likely consequence of the spatial heterogeneity in vegetation composition, successional trajectories, climatic, and geophysical conditions. Our study highlights the spatial complexity of tundra wildfire regimes as well as their impacts on tundra ecosystems. We thus call for greater attention to fire-vegetation interactions in different ecosystems across the circumpolar tundra domain.

Introduction

Located in the high northern latitudes, the circumpolar Arctic tundra is the northernmost terrestrial biome on Earth[1]. Over the past decades, this area has experienced the highest level of warming on land, with a magnitude of nearly three times the global average[2]. Such strong warming has led to a series of profound changes in the Arctic tundra, including the increases in shrub abundance, cover, and biomass[3-5], a phenomenon known as shrubification. Multiple warming-induced drivers are known to contribute to shrubification, including increased air temperatures[6-9], higher nutrient levels[6,10], and improved drainage associated with the thawing of permafrost[6,11,12]. Field studies[3,7,13] and satellite observations[14-16] indicate that shrubification is underway across the circumpolar tundra, which have strong implications for the carbon cycle, energy budget, and other ecosystem properties because shrubs possess different regulatory effects on carbon[17], permafrost[18], albedo[19], and evapotranspiration[20]. Widespread tundra shrubification will likely have substantial regional and global consequences and, therefore, has been a key research focus of the Arctic research community.

Although relatively infrequent[21], wildfires are one of the major disturbance agents in the tundra and are capable of exerting substantial climatic[22] and ecological[23] impacts. Paleorecords show that tundra fire regimes have been much more active at certain points in the past than in the present and it was most likely fueled by the higher dominance of shrubs within the ancient tundra[24]. Considering the substantial Arctic warming and the associated shrubification, the present-day tundra may be reaching a tipping point where fire regimes, which are already believed to be increasingly active[25,26], may be further intensified. A key dynamic in this fire-shrub relationship has been speculated to be a positive feedback loop between shrubs and wildfires[23,27-29]. On the one hand, fires may facilitate shrubification (i.e., leading to more shrub cover or higher shrub biomass compared to the unburned sites). Specifically, fires may create favorable conditions for shrub establishment and growth, including increased mineral soil exposure[13,27], improved drainage[30], higher nutrient availability[10,31], and deeper active layer[13]. On the other hand, shrubs represent a more complex fuel matrix due to their substantially higher biomass and coarseness of fuels compared to herbaceous and non-vascular plants – the only other two components of tundra vegetation. As such, they support longer residence time for flaming fires as well as residual smoldering burning[32,33]. A larger shrub fraction in vegetation composition is, therefore, likely to lead to more spatially extensive and deeper burns[23,27,32], forming a positive feedback loop. The existence of this fire-shrub positive feedback loop has been shown in several local-scale studies[27-29], however, whether this feedback loop operates widely across the Arctic tundra remains unclear. Thus, our understanding of the present-day ecosystem-wide fire regimes and our ability to develop future projections are strongly linked to our understanding of the tundra-wide patterns of fire-shrub relationship beyond local-scale observations.

Tundra is a vast and, arguably, one of the least accessible global biomes which strongly limits the potential for extensive field campaigns. As in most similar cases involving remote and inaccessible areas, satellite observations provide a critical source of information that allows for the extrapolation of the relationships established at local sites to assess ecosystem-wide patterns. In this study, we used Landsat (a 30 m spatial resolution optical system) observations in conjunction with field data collected in different parts of the tundra to examine the relationship between wildfires and shrubs across the Alaskan tundra. Instead of direct measurements of vertical structure, optical observations were used to establish statistical relationships between the observable abundance of photosynthetically active vegetation and plant cover types. We used the annual maximum Normalized Difference Vegetation Index ($NDVI_{max}$), which has been found to be a good indicator of tundra biomass at the local to regional scales[34-41] (although low correlation has been reported due to localized factors[42]), as the primary remotely sensed metric. Although across Low Arctic tundra aboveground biomass load is dominated by shrub biomass[37], $NDVI_{max}$ response is also driven by the presence and abundance of graminoids[16], which also play an important role in tundra ecosystems and are usually the dominant vegetation type during the early recovery stage of post-fire tundra sites[43-45]. Our analysis (Supplementary Fig. 1) compared Landsat-based $NDVI_{max}$ with field-measured fractional shrub and graminoid cover from multiple sites across the four main subregions of Alaskan tundra (Fig. 1) (Loboda, et al. [46] (our data), Macander, et al. [47], and Frost, et al. [48]). The results showed that although a clear contribution from graminoids to $NDVI_{max}$ is evident, a much stronger relationship exists between $NDVI_{max}$ and shrub cover at the landscape level. Thus, in this study, we use satellite-derived assessment of vegetation response ($NDVI_{max}$) to describe the extent and spatial variability of the hypothesized shrub-dominated fire-biomass positive feedback loop across the Alaskan tundra.

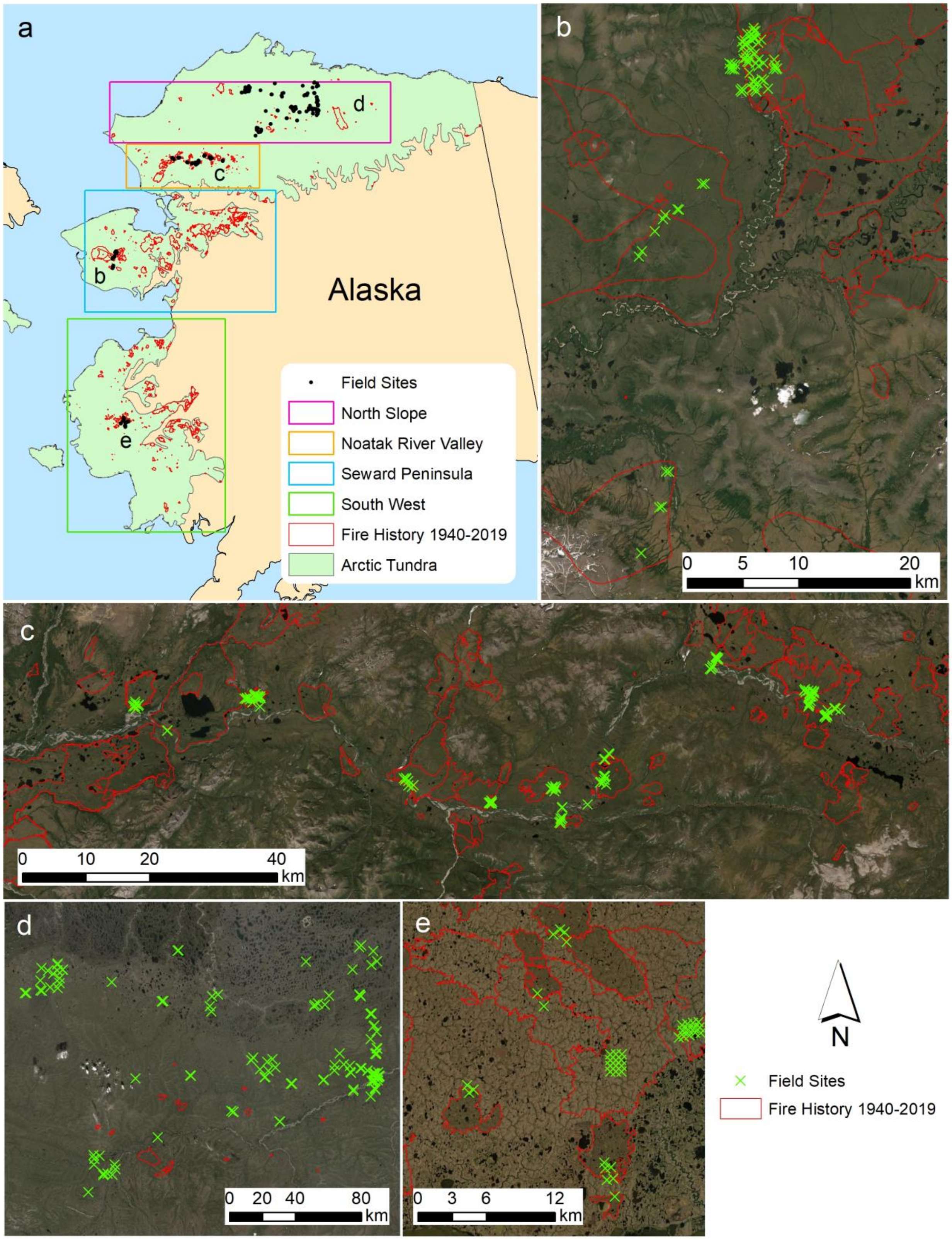

Fig. 1|Distribution of field sites in the context of the Alaskan tundra. Inset a shows the extents of the four subregions used in this study. The boundary of the Arctic tundra is delineated based on the

Circumpolar Arctic Vegetation Map [49] (CAVM). The fire history is based on the Alaska Large Fire Database. Field data in Seward (Inset b) and Noatak (Inset c) were collected by our team[46]. Field data in the North Slope (Inset d) and the South West (Inset e) were collected by Macander, et al. [47] and Frost, et al. [48], respectively.

A fire-biomass positive feedback loop is evident across Alaskan tundra and is strongly related to burn severity

Using the almost 40-year Landsat data record and wildfire history, coupled with a large number of random sample points (accounting for bare ground and water, Supplementary Fig. 2), we established $NDVI_{max}$ anomaly trajectories for the four subregions of the Alaskan tundra: the Noatak River Valley (hereafter referred to as Noatak), the Seward Peninsula (Seward), the North Slope, and the South West (Fig. 2). We found boosting effects of various degrees on the post-fire increases of $NDVI_{max}$ in all four tundra subregions, particularly at sites that have experienced high severity burns (red lines in Fig. 2). In high severity burns within all subregions except for Seward, the initial decrease in $NDVI_{max}$, associated with consumption of aboveground biomass and deposition of char and ash on the surface, gradually dissipates within the first five years after the fire event. Beyond the first five years, post-fire $NDVI_{max}$ of severe burns exceeds that of the unburned control sites (showing a statistically significant difference) throughout our tracking period of ~30 years after a fire event. In Seward, however, we did not detect a notable elevated $NDVI_{max}$ period post-fire even within the high severity burns (the increase in $NDVI_{max}$ anomaly approaching the end of the trajectory in Fig. 2c is not statistically significant). In stark contrast with high severity burned sites, sites that experienced low severity fires (green lines in Fig. 2) exhibit very muted responses in post-fire $NDVI_{max}$. Except for the initial post-fire periods in the North Slope and Noatak, $NDVI_{max}$ values of low severity burned sites are practically indistinguishable from the unburned control sites. As expected, moderate severity burns show post-fire $NDVI_{max}$ patterns that are somewhat between that of the high and low severity burns.

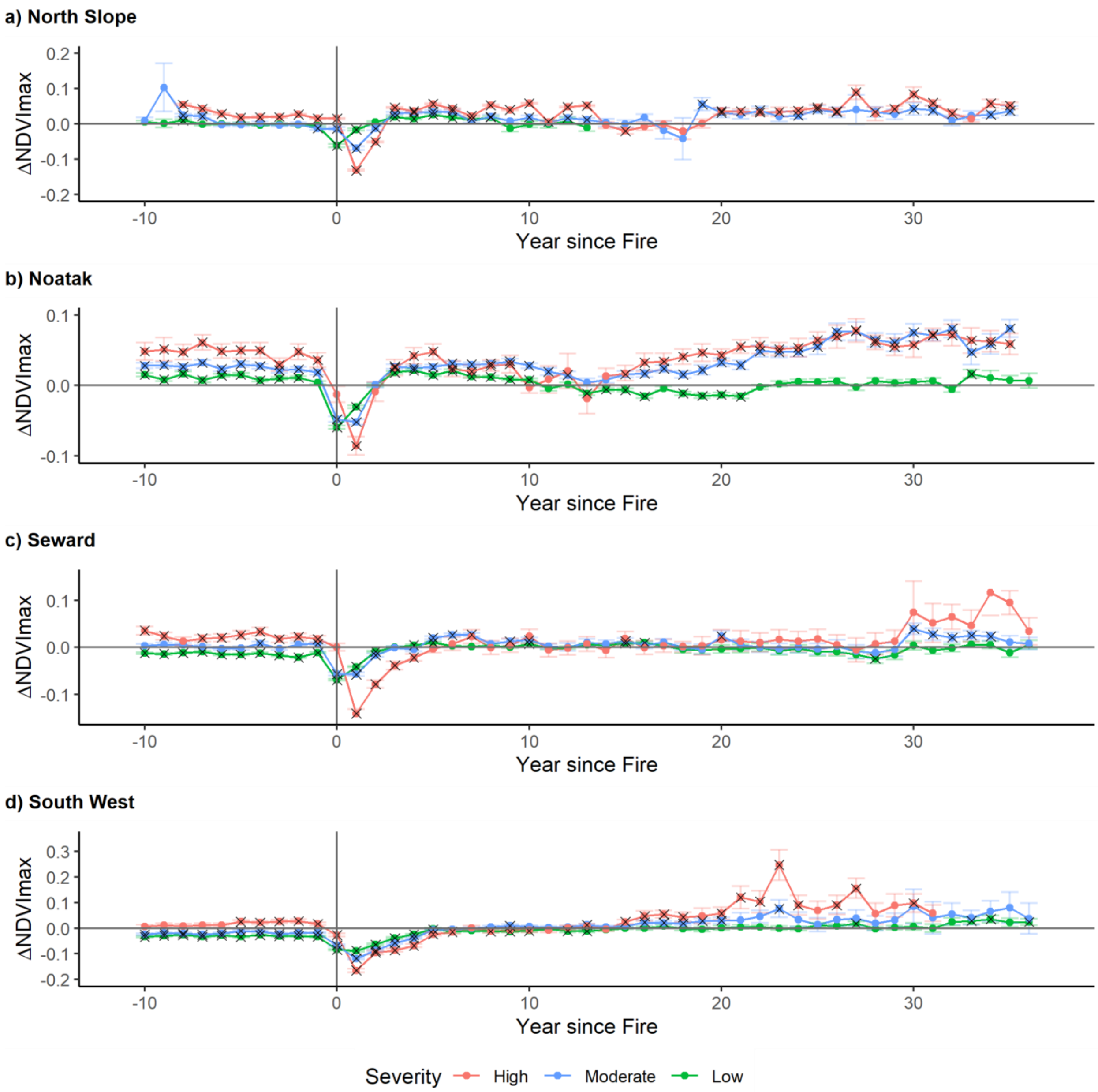

Fig. 2|Post-fire $NDVI_{max}$ anomaly trajectories for different burn severity levels calculated based on annual $NDVI_{max}$ extracted from the random sample points across the Alaskan tundra. Points that are marked by crosses represent the year since fire (YSF) values where the $NDVI_{max}$ values of the burned sites are statistically different from the unburned sites based on paired t-tests ($p<0.05$; two-tailed). Error bars denote ±1 standard error.

Our analysis also revealed that the pre-fire $NDVI_{max}$ values of the majority of high severity burns are higher (at statistically significant levels) than those of the unburned sites in all four subregions (Fig. 2). This indicates that the severity of a fire event is driven by the initial biomass loading of the fire-impacted area. The $NDVI_{max}$ patterns shown during the pre- and post-fire stages, taken together, indicate that a fire-biomass positive feedback loop commonly exists in at least three of the four subregions of the Alaskan tundra (with the exception of Seward). Additionally, we found that, while this fire-biomass feedback loop is fairly common across the Alaskan tundra, it is not ubiquitous. Noticeably, burn severity is both driven by, and a driver of the propagation of the fire-biomass positive feedback loop. Our analysis shows that high severity burns are associated with the largest magnitude of the fire-biomass interactions (i.e., largest numerical differences between burned and unburned sites) in all but one subregion (Fig. 2) and also in both uplands and lowlands. This is significant as the upland and lowland landscapes have different permafrost characteristics known to affect local-scale climate-fire-shrub interactions[29]. These relationships are evident in both the North Slope and Noatak where 30 m landscape type maps are available (Fig. 3). These findings have strong ecological implications as they show that wildfires with higher severity can impose substantially higher impacts on the fire-vegetation interactions in the tundra. In the North Slope, recent fire record (the 1980s – present) is dominated by high severity burns primarily attributable to a single extreme (both in extent and impact) fire event - the 2007 Anaktuvuk River Fire. As a result, the overall $NDVI_{max}$ anomaly trajectory of all burned sites in the North Slope (Supplementary Fig. 3a) resembles that of the high severity burned sites only (Fig. 2a). In contrast, at sites that have experienced lower severity fires, the weaker fire-induced effects may not be sufficient to impose substantial and long-lasting impacts on the existing ecological successions and a positive feedback loop does not emerge.

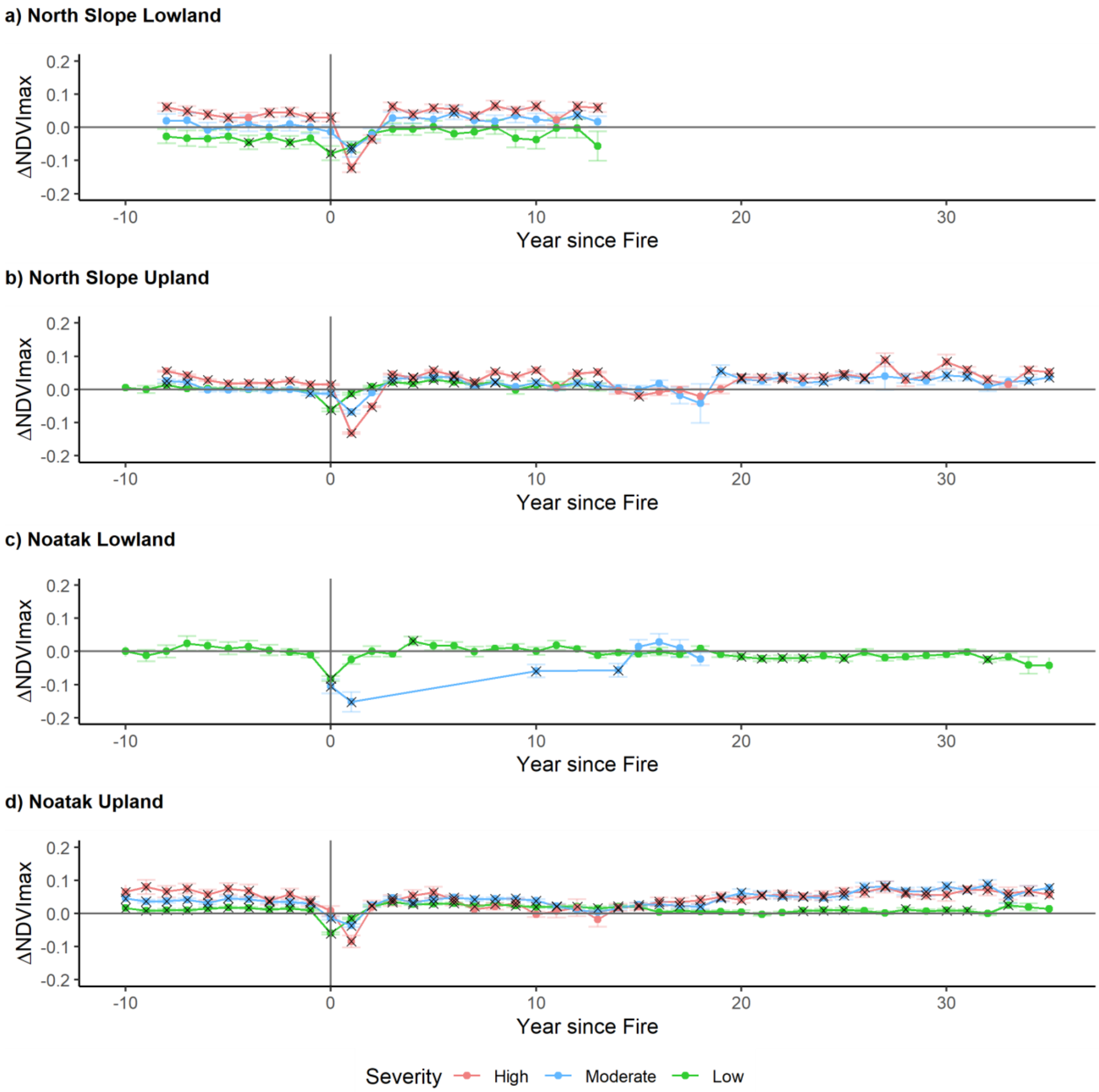

Fig. 3 | Post-fire $NDVI_{max}$ anomaly trajectories for different landscape types (according to Muller, et al. [50], which is only available for Noatak and North Slope) and for different burn severity levels. Points that are marked by crosses represent the YSF values where the $NDVI_{max}$ values of the burned sites are statistically different from the unburned sites based on paired t-tests ($p<0.05$; two-tailed). Error bars denote ±1 standard error.

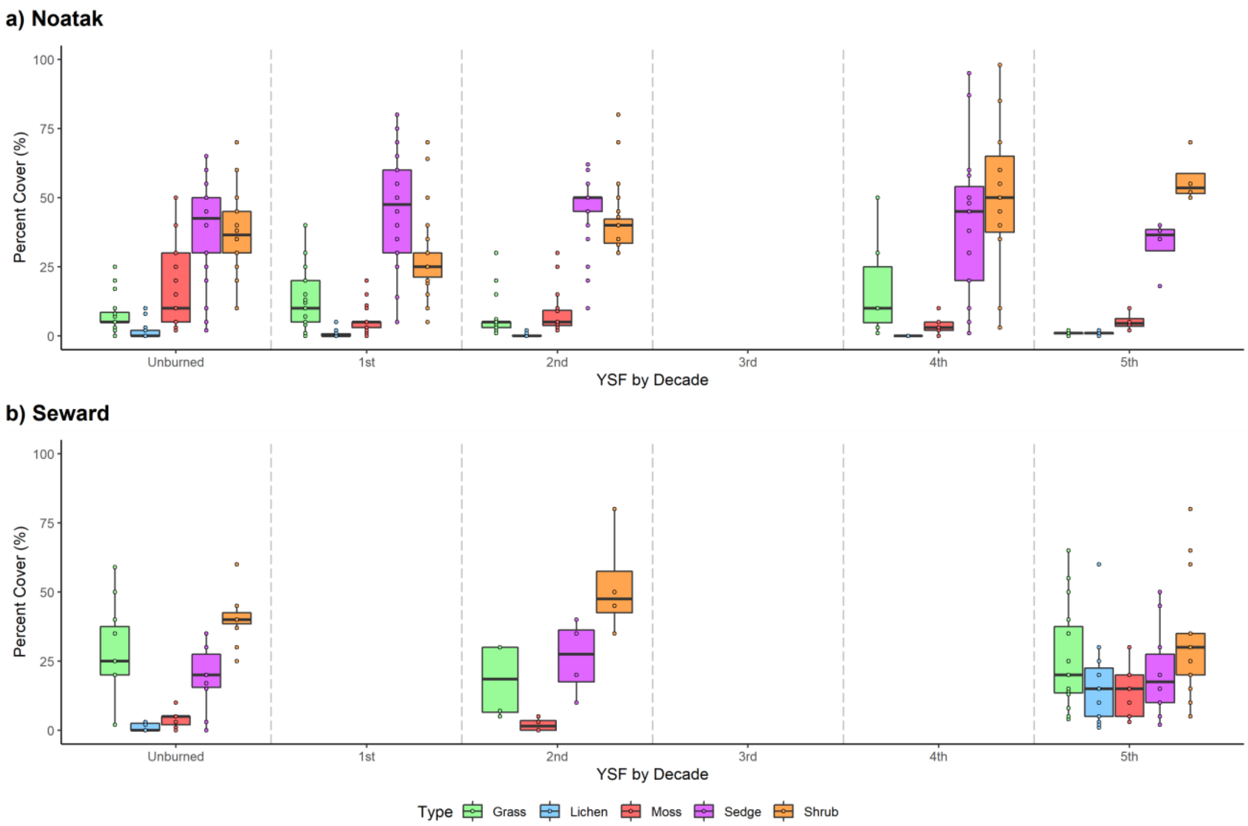

Fig. 4 | Boxplots showing the relationship between YSF and vegetation cover (in %) according to our ocular assessment of vegetation cover over all 10-m × 10-m sites. Each circle indicates an observation. The YSF values for the burned sites are classified into five classes by decade (e.g., observations whose YSF are between 1 and 10 are summarized into the 1^{st}-decade bin).

Untangling vegetation shifts underpinning the variability of the satellite-observed fire-biomass positive feedback loop

Even though a fire-biomass positive feedback loop is evident across the Alaskan tundra as a whole, we found that its presence and magnitude vary substantially both within and between the subregions. Noatak and Seward are the two tundra subregions with very active recent histories of burning[21] and of similar Erect-shrub Tundra physiognomic type (according to the CAVM dataset[51]). However, the post-fire $NDVI_{max}$ anomaly trajectories (Fig. 2 and Fig. 5) between these two subregions show clear divergent patterns. In Noatak, at the majority of burned sites (including both high and moderate severity sites), post-fire $NDVI_{max}$ increases significantly over unburned control sites (Fig. 2). This elevation of $NDVI_{max}$ lasts for decades until the end of the tracking period. In contrast in Seward, no statistically significant increase in post-fire $NDVI_{max}$ is detected not only at high severity burned sites (Fig. 2), but also high severity burned sites of all three main physiognomic types (i.e., Erect-shrub Tundra, Graminoid Tundra, and Wetland; Fig. 5). With the exception of the few years immediately after the fires, post-fire NDVI$_{max}$ of most burns in Seward are practically indistinguishable from that of unburned sites.

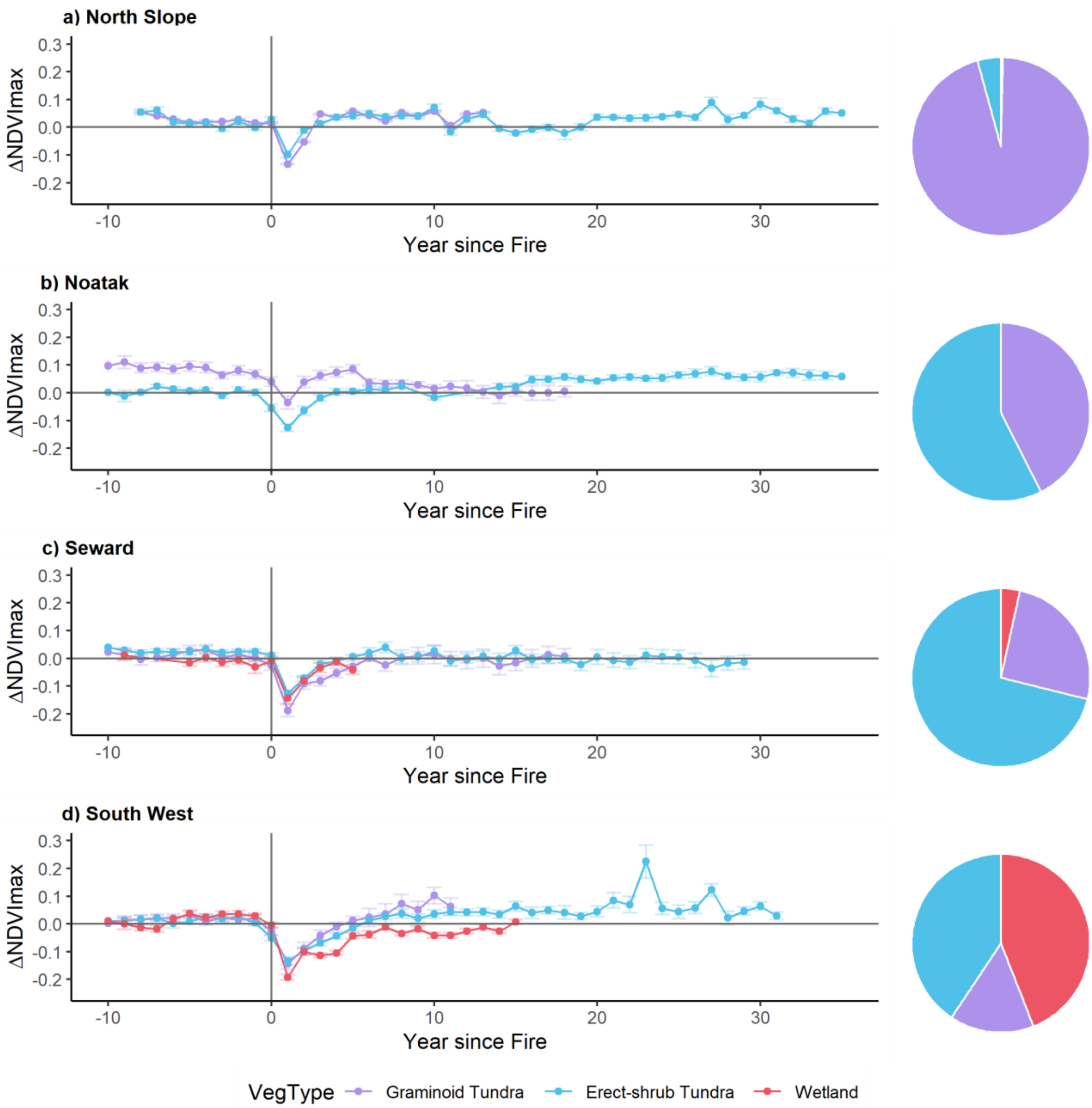

Fig. 5 | Post-fire NDVI$_{max}$ anomaly trajectories for different physiognomic types (according to the 1 km CAVM raster dataset [51]) and for high severity level burned points. Error bars denote ±1 standard error. The pie charts on the right show the relative proportions of the different physiognomic types among all high severity burned points in the corresponding subregion.

Over a 3-year period (2016 – 2018), we conducted extensive field sampling data collection within a chronosequence of burns in Noatak and Seward tundra. An explicit aim of the data collection was to acquire high-level observation of vegetation composition within a large number of burns of different ages and burn severity (Fig. 1b-c) to assess post-fire vegetation recovery patterns over five decades using the space-for-time substitution approach. The dataset includes two metrics: 1) a 10-m × 10-m plot ocular assessment of fractional vegetation cover (shrub, grass, sedge, moss, lichen) and 2) a 1-m × 1-m plot of fractional assessment of shrub cover as well as shrub species, stem count and stem diameter measurements. We found that recovery patterns observed in the field data at both the 10-m × 10-m (Fig. 4) and the 1-m × 1-m plot levels (Fig 6d) are highly consistent with our remote sensing-based analysis. At the landscape scale (i.e., 10 m plots, Fig. 4), we detected a continuous increase in shrub cover following fire occurrence in Noatak and by the fifth decade, post-fire sites are dominated by shrubs. In Seward, on the contrary, the burns show an increase in shrub cover initially after the fires, but shrub cover drops to slightly below the unburned level by the fifth decade. Analysis at the finer scale (1-m × 1-m plots) tells a similar but more detailed story. In Noatak, shrub biomass substantially increases since the fires whereas, in Seward, shrub biomass experiences a minor increase in the second decade after the fires then decreases to the unburned level by the fifth decade (Fig. 6a). Our detailed measurements coupled with generalized linear models reveal a series of important insights (Supplementary Table 1). In Noatak, shrub biomass initially recovers through rapid re-establishment of shrubs, dominated by *Ledum spp.* with stem diameter between 1 and 3 mm. As the shrubs mature, in the second decade, the total number of individual stems decreases but their diameter (not shown), shrub height, and shrub cover continue to grow with the overall dominance of dwarf birch (*Betula nana*) (Supplementary Table 2). In Seward, we observed a nearly identical pre-fire shrub biomass but a different post-fire trajectory which results in no discernable increase in shrub cover, shrub height, and total biomass over time. Although *Ledum* and *Betula* shrubs are present, in Seward, shrub biomass is dominated by willows (*Salix spp.*) (Supplementary Table 2). These results indicate that the tundra in Seward is more resilient to wildfires in a way that post-fire tundra is able to recover to a status that more or less resembles the pre-fire unburned conditions. The tundra in Noatak, however, is more vulnerable to wildfires –

moderate- and high-severity levels of wildfires are capable of greatly boosting the role played by shrubs in the post-fire stands.

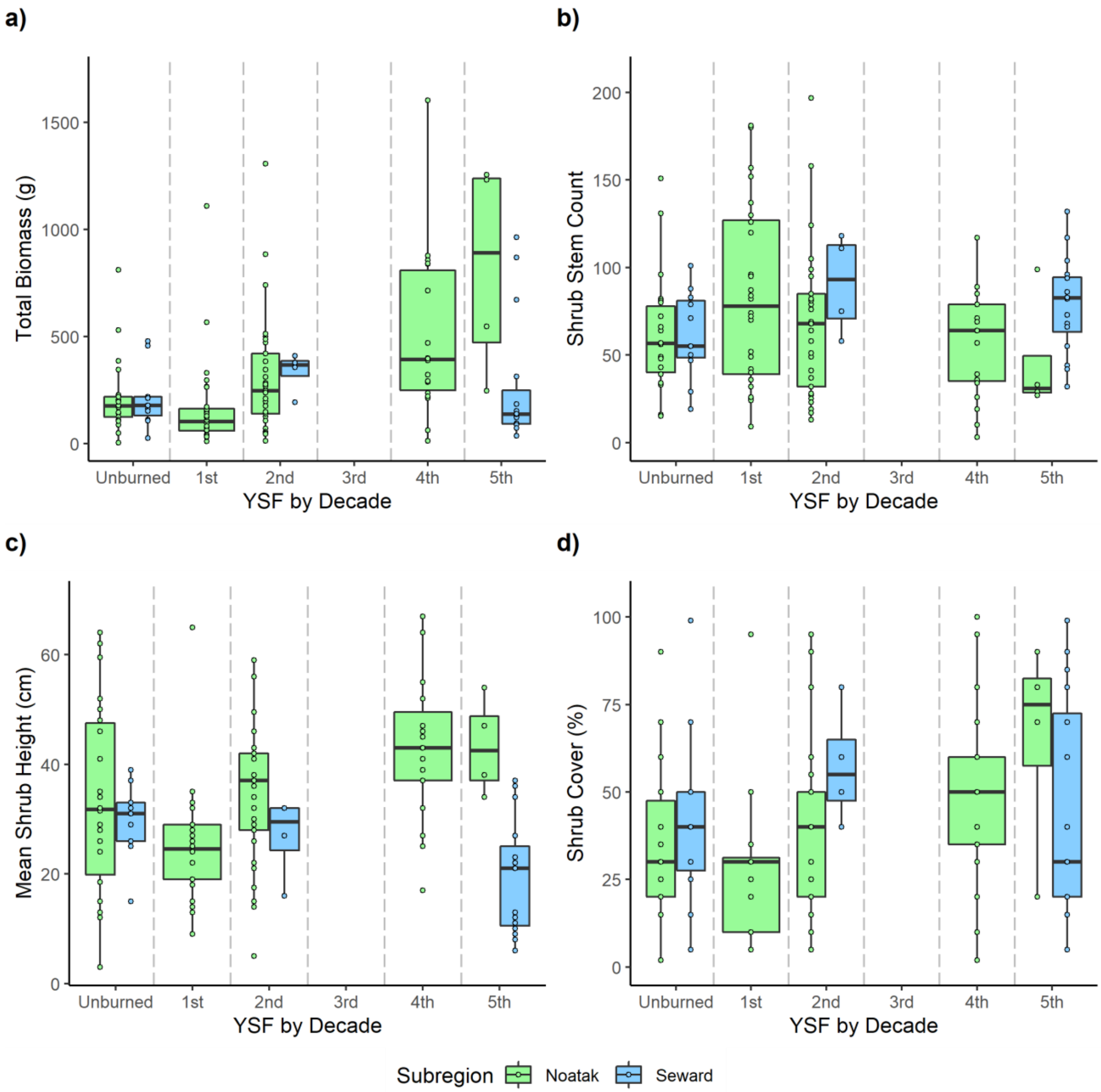

Fig. 6 | Boxplots showing the relationship between YSF and total shrub biomass (top-left), total stem count (top-right), mean shrub height (bottom-left), and percent shrub cover (bottom-right) as measured in all 1-m × 1-m sites. Each circle indicates an observation.

Implications of common but non-uniform fire-biomass feedback loop across the Alaskan tundra in the context of climate change

Tundra wildfires have received less attention from the scientific community and general public because of their relative infrequency and low direct impacts on human populations. However, the expected increases in fire extent, frequency, and severity[25,52,53], coupled with the crucial role of circumpolar tundra in global climate change, renders understanding tundra fires better an urgent and strategically important matter. Previous studies, notably Camac, et al. [27], Gaglioti, et al. [28], and Chen, et al. [29], have shown that a fire-shrub positive feedback loop exists at the local scales in the tundra. Our results have established the prevalence of this phenomenon across the Alaskan tundra. It is likely that this feedback loop is dominated by shrubs, although a minor and possibly more transient role is also played by graminoids. In addition, we show that most tundra wildfires, especially those with higher severity, lead to continued shrub dominance, which, in turn, provides higher fuel loads and increases the probability of severe impact. These findings have profound implications in the context of climate change. Under the strong Arctic warming, most of the Arctic tundra biome is experiencing substantial "greening" and shrubs are a major contributor to this process[7,16,54]. Even though both warming and wildfire have been suggested to boost the shrubification, our results show that during the 15-year period between 2006 and 2020, the increases in $NDVI_{max}$ at the high severity burned sites (indicated by the red lines in Fig. 7) are similar to the mean $NDVI_{max}$ differences as observed between the high severity burned sites and the background sites (indicated by the blue lines in Fig. 7). This means that at least during the recent decades, high severity fires promote the shrubification process at a magnitude that is on par with that of the warming-induced shrubification. Considering future projections of increases in wildfire occurrence, extent, and severity in the high northern latitudes[26,52], the strong boosting effect of high severity fires on shrubification as we have shown is likely to translate into substantial impacts on the species composition and successional trajectory of tundra ecosystems towards an accelerated shrubification of this biome.

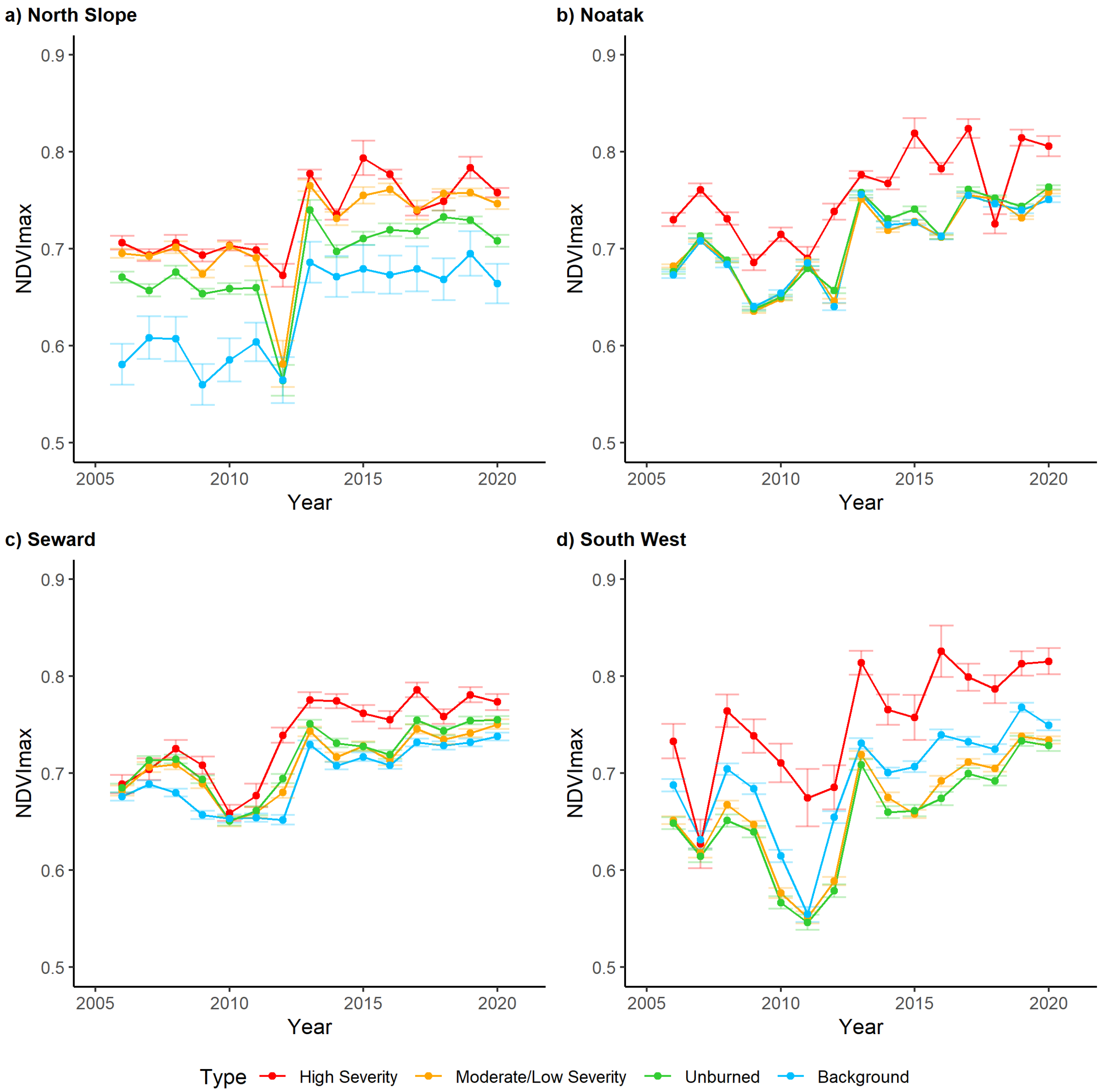

Fig. 7| $NDVI_{max}$ trajectories between 2006 and 2020 based on matching burned, unburned, and background sample points. Error bars denote ±1 standard error.

The divergence in the post-fire recovery patterns between Noatak and Seward, which as our field data indicate is owing in part to the different species compositions and successional trajectories, indicates that some tundra ecosystems are more resilient to wildfires than others. We would like to stress that this "resilience" may translate into the difficulty to initiate and sustain wildfires for some ecosystems, but for other ecosystems (including those in Seward), it may mean the ability to recover from fires. In either case, this means that despite the ongoing strong Arctic warming, the intensification of wildfire regimes and the transformation of dominant vegetation species may not be the inevitable future for all of the Arctic tundra. Graminoid-dominated tundra, which is more prone to repeat burns and more adaptive to fire regimes with high fire frequency[21,55,56], may still be a significant component of the tundra biome in the future.

It has become increasingly clear that the Arctic tundra, despite being seemingly homogeneous, is in fact quite variable at the spatial scales that affect ecosystem functioning. This is reflected by the spatial heterogeneity in species compositions[51,54], geophysical conditions[57,58], and the resultant vegetation-land-climate interactions[16,58-63]. Comparatively, we have a much poorer understanding of the role played by wildfires in tundra ecosystems. In terms of wildfire distribution, which is the foundation for assessing and projecting wildfires' ecological and climatic impacts at large spatial scales, we do not yet have a clear picture of the spatio-temporal distribution of tundra wildfires across the circumpolar tundra domain except for the post-2000 era[64]. Even in regions like Alaska, where wildfire history exists since the 1940s and is well-maintained[65], is shown to have notable omissions when it comes to reporting tundra wildfires[66]. A combination of factors including a lack of reliable long-term tundra wildfire records, tundra's extreme environmental conditions and subsequent lack of access, tundra wildfires' remoteness, and relative infrequency, have led to the fact that wildfires' impacts on tundra ecosystems have remained understudied. Here we focused on the Alaskan tundra, which has been a hotspot of wildfires across the circumpolar tundra domain over the past 20 years[64]. Our study shows that all four subregions of the Alaskan tundra exhibit certain degrees of dissimilarity from others based on $NDVI_{max}$ alone. This highlights the substantial heterogeneity within the Arctic tundra in terms of the fire-vegetation interactions which is likely a consequence of the spatial variabilities of the climate, vegetation, and geophysical conditions. Even though our field surveys are able to provide critical ecological contexts for some of the patterns that our large-scale analyses have revealed, our discoveries prompt further questions many of which we are yet to be able to answer. For example, what drives the $NDVI_{max}$ trajectories in other tundra subregions? What impact does fire occurrence has on vegetation recovery of the South West subregion, which is known to be a unique division of the Alaskan tundra for its dominance of lichen and wetlands[67] and where $NDVI_{max}$ trajectories of moderate and low severity burns are lower than the unburned control (Figs. 2 and 5), which, in turn, are lower than the background sites (Fig. 7)? Do these patterns in the South West reflect the implications of different hydrological regimes and could they become more widespread across the entire tundra domain which is predicted to be wetter in the future[68,69]? Is the increasing dominance of shrubs as observed in Noatak a transient or permanent pattern? What level of climate change and associated changes in the biogeophysical conditions will be sufficient to overcome the resilience as exhibited in areas like Seward? While recent studies in the Arctic domain can allow us to put forth some hypotheses for these questions, substantially more work in this domain is needed to develop an understanding of the guiding processes. In light of this, we would like to advocate for more field campaigns and prescribed burns in a variety of tundra ecosystems. Currently, there is a great imbalance between the distribution of studies involving fire-related field data in the tundra. At the circumpolar level, most studies concentrate on the Alaskan tundra, whereas within the Alaskan tundra, at least half of the studies in the English literature over the past decade have focused on the 2007 Anaktuvuk River Fire (according to our literature review). Even though severe events such as the Anaktuvuk River Fire is critically important to our understanding of future tundra fire regimes due to the expected increase in tundra fire severity[22,25], most tundra fires are of moderate to low severity and our study has shown that they lead to considerably different impacts to the tundra than the severe ones. In addition, many tundra fires occur in ecosystems that are drastically different from the North Slope, which the Anaktuvuk River Fire was located in. Therefore, it is crucial to have more observations in a great variety of burned sites with various wildfire histories, species compositions, and geophysical conditions. In addition to more field campaigns, prescribed burns and controlled experiments would allow us to understand tundra fires better similar to the knowledge gains from those in boreal forests[70-72]. Overall, an improved understanding of the variations in the fire-vegetation interaction across the Arctic tundra will facilitate the development of Earth system models with better performance, which, in turn, allow us to better estimate the consequences that come with a changing tundra.

Methods

Field data collection

We conducted field measurements during three field campaigns to the Alaskan tundra between July and August of 2016-2018, among which Noatak was visited twice and Seward was visited once. The field sites that we visited were determined prior to our field trips based on a stratified randomized scheme taking into account a combination of factors including drainage (calculated based on the U.S. Geological Survey Interferometric Synthetic Aperture Radar (IFSAR) Digital Elevation Model data), year since the last fire (calculated based on the Alaska Large Fire

Database; ALFD), and burn severity (represented by the Burn Severity Index (BSI), which was calculated based on post-fire Normalized Burn Ratio (NBR) following Loboda, et al. [73]. A surplus of potential field sites was generated during the planning stage and it was up to the field team to determine which sites to visit based on the time limit and accessibility of the sites when there were in the tundra. The field team also decided the locations of the unburned sites, i.e., sites that shared similar surface conditions as the burned sites but had not experienced known fires. Eventually a total of 137 sites (Noatak: 83 burned + 22 unburned; Seward: 21 burned + 11 unburned) that were confirmed to have only burned once since the 1970s were visited during the three campaigns. At each site, the field team conducted measurements for a series of vegetation-related parameters at two different scales. We established one 1-m × 1-m plot within which we estimated the shrub cover, counted the number of shrub species as well as the number of stems of each species. We also estimated the biomass of the shrubs found within the 1-m × 1-m plot by applying the allometric equations developed by Smith and Brand [74] which relate basal diameters to biomass. In addition, mean shrub height and percent shrub cover were measured and estimated, respectively. Another 10-m x 10-m plot (which enclosed and shared a corner with the 1-m × 1-m plot) was also established at each site, where we estimated the percent cover of the main vegetation types found within the plot based on an ocular assessment.

$NDVI_{max}$ vs. fractional cover of shrubs and graminoids

Our primary aim is to confirm that the common satellite-based observation of vegetation greenness ($NDVI_{max}$) is representative of conditions in the Alaskan tundra and can be used reliably to assess ecosystem-wide changes and make inferences about vegetation composition. We combined field datasets that were collected in the North Slope[47] and the South West[48], respectively, with our own field data from Noatak and Seward (described in the previous section). These field data included *in situ* assessments of shrub and graminoid cover. Due to the difference in the vegetation classification systems that are used by these three datasets, a vegetation class reconciliation was carried out to ensure the reconciled datasets all have a single "shrub" and a single "graminoid" class (for our field data, grasses and sedges were considered graminoids; for Macander, et al. [47] and Frost, et al. [48], deciduous shrubs and evergreen shrubs were merged into the shrub class and sedges, rushes, and grasses were merged into the graminoid class), followed by a merger of the three datasets. $NDVI_{max}$ for each field plot of the merged dataset was then extracted on Google Earth Engine (GEE) based on the Landsat surface reflectance data[75,76] for June-August in the corresponding year.

For example, $NDVI_{max}$ for 2012 was extracted for field plot A if the *in situ* data at field plot A was collected in 2012. Simple linear regression was implemented between $NDVI_{max}$ and recorded shrub and graminoid cover for all four subregions (Supplementary Fig. 1).

Extraction of $NDVI_{max}$ and $NDVI_{max}$ anomaly trajectories

For our domain-wide analysis, annual $NDVI_{max}$ values were extracted at randomly generated sample points across the Alaskan tundra. Three types of random sample points - burned, unburned, and background - were created. Burned sample points were generated within areas that have experienced burning between 1985 and 2017 as reported by Monitoring Trends in Burn Severity (MTBS) product[77]. We adopted MTBS because it not only provides human-guided identification of burned areas within burn scars that are larger than 400 ha in Alaska, but also the burn severity levels (i.e., low, moderate, and high) of burn areas within the scars. Areas that experienced more than one fire during 1985-2017 were excluded to minimize the compounding effect that repeated burns may have on the post-fire vegetation recovery. Unburned sample points were generated within the buffered zone (determined as the areas between two buffer distances - 50 m and 1,000 m - from each burn scar) of the burn scars. Each unburned point was matched to a burned point from the same burn scar (to allow for $NDVI_{max}$ anomaly calculation). Background sample points were generated within the areas across the four tundra subregions that are below 300 m above sea level (our previous unpublished results showed that less than 7% of burned areas since the 1940s in Alaskan tundra occurred above the 300 m line). For each burned point, an unburned point (from the same burn scar) and a background point were matched, resulting in a three-point trio. Overall, we generated 5,000 trios for each subregion, leading to a total of 60,000 sample points for the entire Alaskan tundra (shown in Supplementary Fig. 2).

Prior to being used to extract $NDVI_{max}$ on GEE, the random sample points were checked against a water mask produced based on the 30 m Global Surface Water (GSW) dataset[78]. To minimize the negative influence of water on NDVI calculation[79], we intentionally created a very liberal water mask. To that end, we buffered all water pixels with >50% of water occurrence as identified by GSW for 90 m (3 Landsat pixels). If any one of the three sample points of the same trio was found to overlap with the water mask, the entire trio was excluded from subsequent analyses. The remaining sample points were used to extract annual $NDVI_{max}$ values based on all Landsat data between 1985 and 2020.

The extracted $NDVI_{max}$ data (which included more than 1 million unique $NDVI_{max}$ retrieves) were subjected to two analyses. The first analysis centered on the establishment of the $NDVI_{max}$

anomaly trajectories. In specific, for each burned sample point, its $NDVI_{max}$ anomaly for a given year (i.e., any year between 1985 and 2020) was calculated by subtracting the $NDVI_{max}$ value of its matched unburned point for the same year from its $NDVI_{max}$ value. For example, if the $NDVI_{max}$ values of burned sample point A and its matched unburned sample point B for year 1985 were 0.622 and 0.543, respectively, the $NDVI_{max}$ anomaly value for point A in 1985 was 0.079. An $NDVI_{max}$ anomaly trajectory was created for each subregion by calculating and plotting the average $NDVI_{max}$ anomaly values of the burned points for each YSF value, calculated as $Year_{observation}$-$Year_{fire}$. In addition to the overall $NDVI_{max}$ anomaly trajectories (which incorporated all burned sample points; Fig. 2), we also took into account burn severity, landscape, and physiognomic types in the trajectory establishment. In specific, we divided all burned samples into groups based on their burn severity levels (i.e., high, moderate, and low; as indicated by the MTBS dataset), landscape types (i.e., Upland, Lowland; as indicated by Muller, et al. [50]), and physiognomic types (i.e., Graminoid Tundra, Erect-shrub Tundra, and Wetland; as indicated by the 1 km CAVM raster dataset[51]) and calculated $NDVI_{max}$ anomalies separately for each of the categories.

The second analysis focused on assessing the post-fire increases in greenness in the context of the warming-induced greening across the tundra over the past decades. We located all burned sample points that experienced burning between 1985 and 2000 (according to MTBS) and calculated their $NDVI_{max}$ trajectories during 2006-2020. A 5-year gap between 2001 and 2005 was implemented intentionally because our $NDVI_{max}$ anomaly trajectories showed that most post-fire decreases in $NDVI_{max}$ tend to disappear within 5 years. For these burned points, we also calculated the 2006-2020 $NDVI_{max}$ trajectories based on the corresponding unburned and background sample points. These trajectories were plotted together to highlight their similarities and differences.

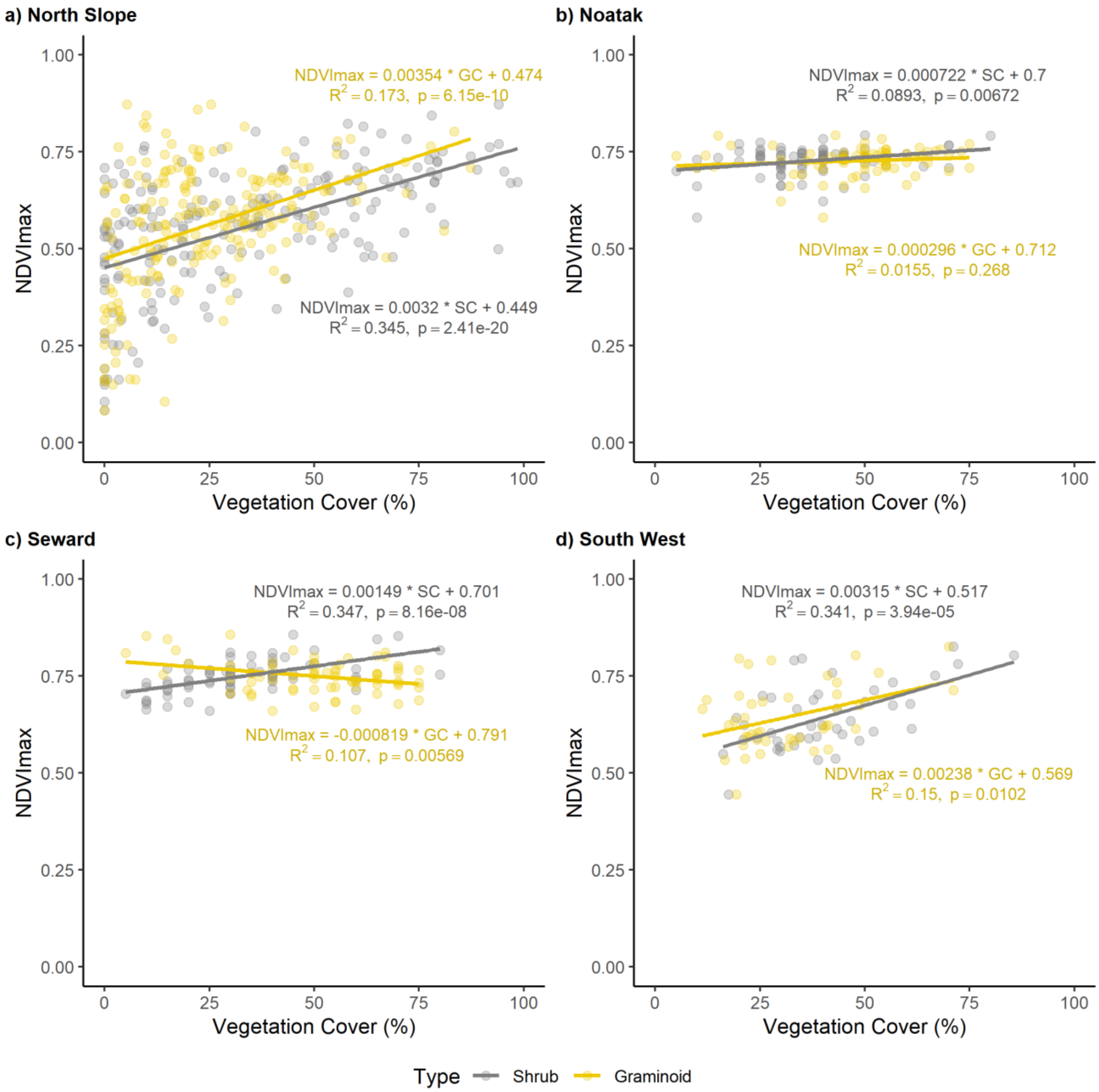

Supplementary Fig. 1 | Scatterplots generated based on field-measured shrub and graminoid cover and NDVI$_{max}$ from the corresponding years as calculated based on Landsat imagery on GEE. Field data for Noatak and Seward were acquired by our team. Field data for North Slope and the South West were acquired by Macander, et al. [47] and Frost, et al. [48], respectively. SC: shrub cover. GC: graminoid cover.

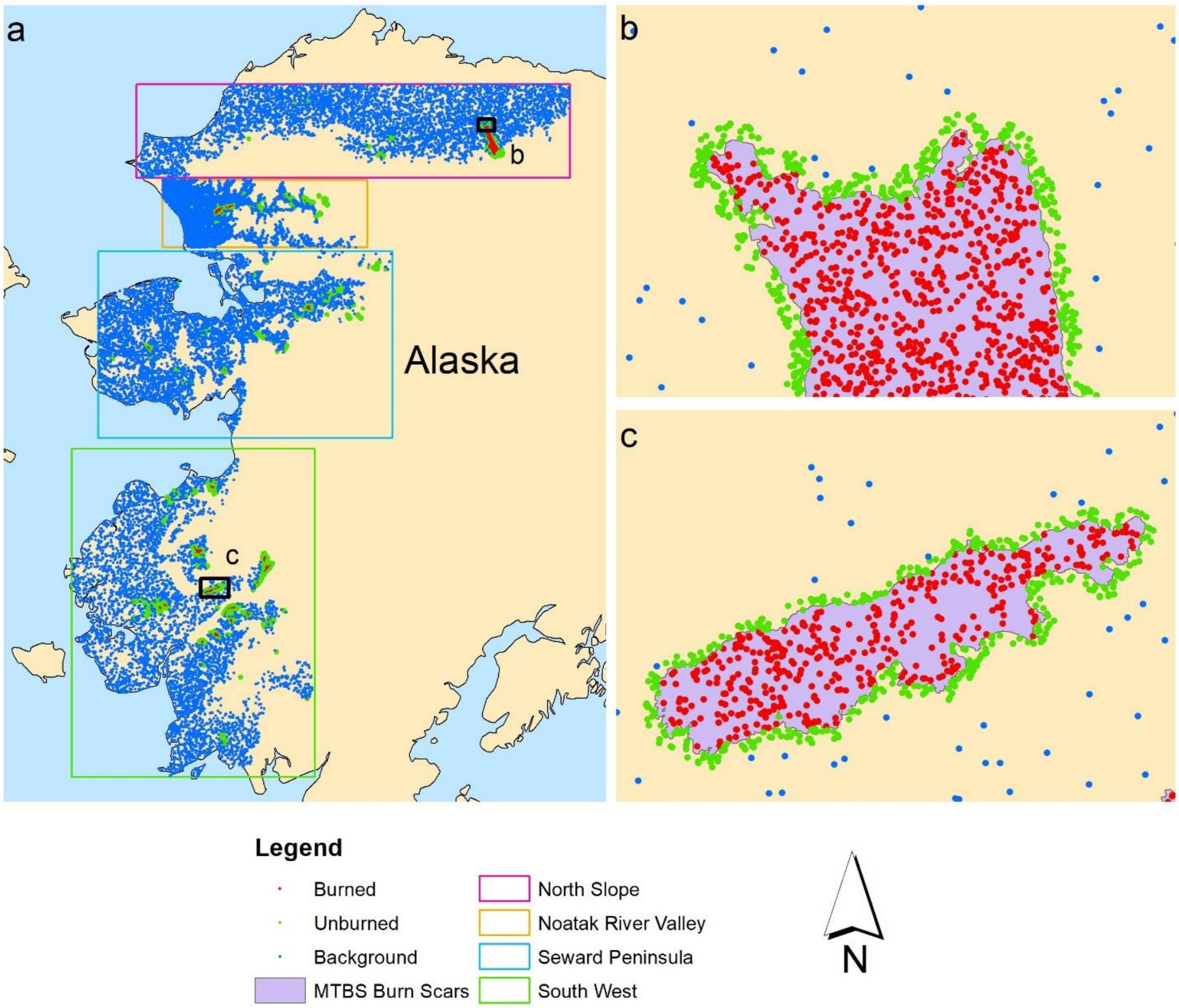

Supplementary Fig. 2|Distribution of random sample points generated across the Alaskan tundra.

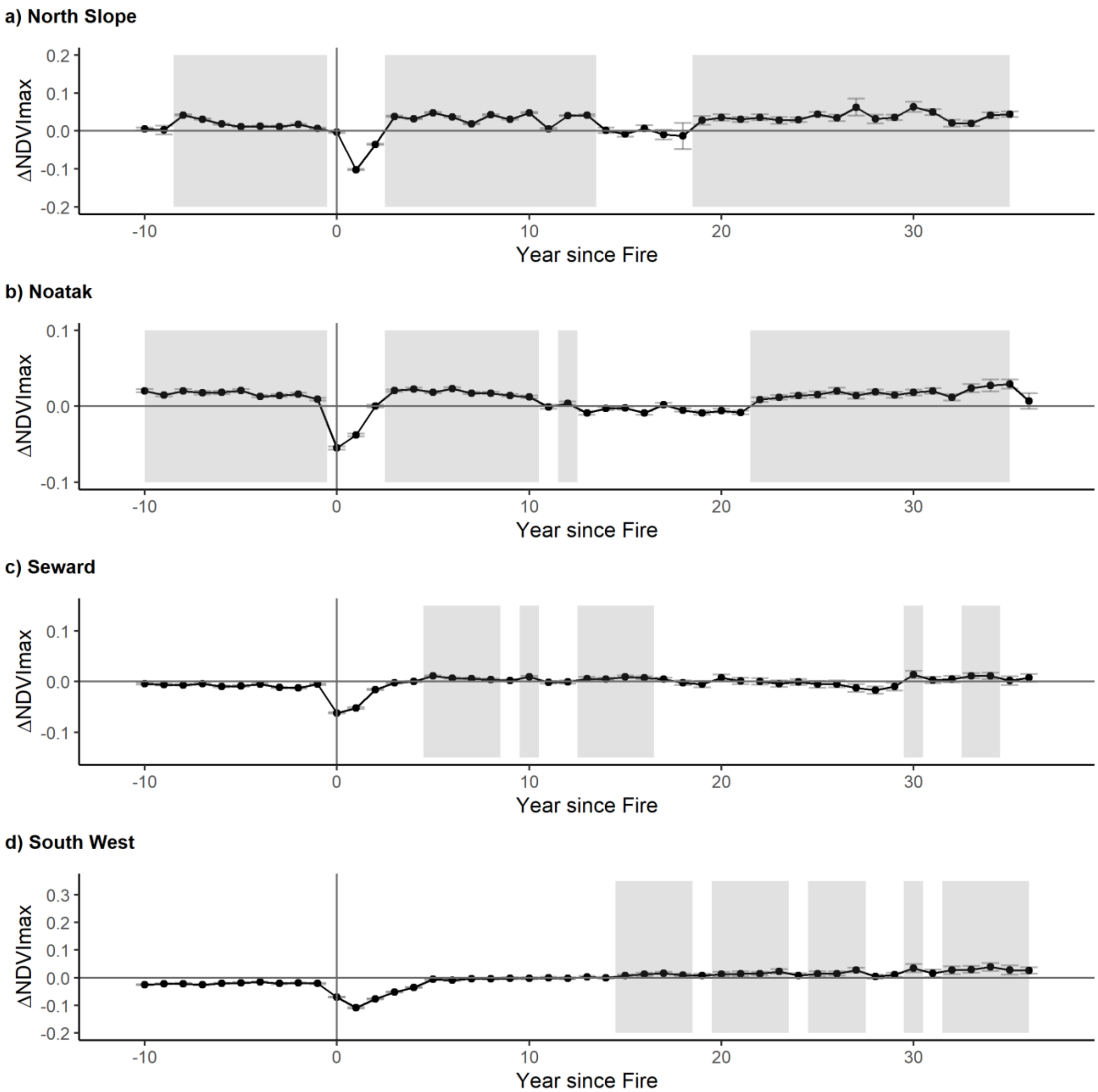

Supplementary Fig. 3|Post-fire $NDVI_{max}$ anomaly trajectories calculated based on annual $NDVI_{max}$ extracted from the random burned and unburned sample points across the Alaskan tundra. Areas highlighted in gray represent the Year since Fire (YSF) values where the $NDVI_{max}$ values of the burned sites are statistically larger than the unburned sites based on paired t-tests ($p<0.05$; one-tailed). Error bars denote ±1 standard error.

Supplementary Table 1. Results of two generalized linear models fitted based on field data collected in Noatak and Seward, respectively. The dependent variable is total shrub biomass, and the independent variables are shrub stem count, fractional shrub cover, mean shrub height, and YSF. Numbers in bold correspond to the variable with the highest importance in each model.

	Variable	Standardized Coefficients	t	Sig.	Model R^2
Noatak	Shrub Stem Count	-0.1342	-1.86773	0.066	0.695
	Shrub Cover	**0.730424**	**8.356773**	**0.000**	
	Mean Shrub Height	0.049605	0.555551	0.580	
	YSF	0.149262	1.9329	0.057	
	(Constant)		-1.47287	0.145	
Seward	Shrub Stem Count	0.042378	0.346451	0.734	0.797
	Shrub Cover	0.099827	0.583279	0.568	
	Mean Shrub Height	**0.817742**	**4.955143**	**0.000**	
	YSF	0.176068	1.469426	0.162	
	(Constant)		-2.40511	0.030	

Supplementary Table 2. Pearson correlation statistics calculated between total shrub biomass and biomass of dwarf birch and willow in Noatak and Seward. N stands for the number of samples that were used in each calculation, with each sample corresponding to a 30 m x 30 m pixel. Numbers in bold indicate the highest Pearson correlation coefficient in each group.

	Dwarf Birch Biomass			Willow Biomass		
	Pearson Correlation	Sig. (2-tailed)	N	Pearson Correlation	Sig. (2-tailed)	N
Total Shrub Biomass (Noatak)	**0.975**	0.000	94	0.147	0.235	67
Total Shrub Biomass (Seward)	0.339	0.098	25	**0.989**	0.000	10

Data Availability

The field data that this study is available through the Oak Ridge National Laboratory Distributed Active Archive Center (ORNL DAAC): https://doi.org/10.3334/ORNLDAAC/1919. All data (including field data) and code (Python, R, IDL, Google Earth Engine) that support the results of this study are available at https://github.com/dchengeo/tundra_fire_shrub_manuscript.

References

1 Olson, D. M. *et al.* Terrestrial ecoregions of the worlds: A new map of life on Earth. *Bioscience* **51**, 933-938, doi:https://doi.org/10.1641/0006-3568(2001)051[0933:teotwa]2.0.co;2 (2001).

2 AMAP. Arctic Climate Change Update 2021: Key Trends and Impacts. Summary for Policy-makers. 16 (Arctic Monitoring and Assessment Programme (AMAP), Tromsø, Norway, 2021).

3 Elmendorf, S. C. *et al.* Plot-scale evidence of tundra vegetation change and links to recent summer warming. *Nature Clim. Change* **2**, 453-457, doi:http://www.nature.com/nclimate/journal/v2/n6/abs/nclimate1465.html#supplementary-information (2012).

4 Sturm, M., Racine, C. & Tape, K. Climate change: Increasing shrub abundance in the Arctic. *Nature* **411**, 546-547, doi:http://dx.doi.org/10.1038/35079180 (2001).

5 Chapin, F. S. *et al.* Role of land-surface changes in Arctic summer warming. *Science* **310**, 657-660, doi:http://dx.doi.org/10.1126/science.1117368 (2005).

6 Mekonnen, Z. A. *et al.* Arctic tundra shrubification: A review of mechanisms and impacts on ecosystem carbon balance. *Environ. Res. Lett.* **16**, 053001, doi:https://doi.org/10.1088/1748-9326/abf28b (2021).

7 Walker, M. D. *et al.* Plant community responses to experimental warming across the tundra biome. *Proc. Natl. Acad. Sci. USA* **103**, 1342, doi:http://dx.doi.org/10.1073/pnas.0503198103 (2006).

8 García Criado, M., Myers-Smith, I. H., Bjorkman, A. D., Lehmann, C. E. R. & Stevens, N. Woody plant encroachment intensifies under climate change across tundra and savanna biomes. *Glob. Ecol. Biogeogr.* **n/a**, doi:https://doi.org/10.1111/geb.13072 (2020).

9 Elmendorf, S. C. *et al.* Global assessment of experimental climate warming on tundra vegetation: heterogeneity over space and time. *Ecol. Lett.* **15**, 164-175, doi:https://doi.org/10.1111/j.1461-0248.2011.01716.x (2012).

10 Mack, M. C., Schuur, E. A. G., Bret-Harte, M. S., Shaver, G. R. & Chapin, F. S. Ecosystem carbon storage in arctic tundra reduced by long-term nutrient fertilization. *Nature* **431**, 440-443, doi:http://www.nature.com/nature/journal/v431/n7007/suppinfo/nature02887_S1.html (2004).

11 Lloyd, A. H., Yoshikawa, K., Fastie, C. L., Hinzman, L. & Fraver, M. Effects of permafrost degradation on woody vegetation at arctic treeline on the Seward Peninsula, Alaska. *Permafrost Periglacial Process.* **14**, 93-101, doi:http://dx.doi.org/10.1002/ppp.446 (2003).

12 Lantz, T. C., Kokelj, S. V., Gergel, S. E. & Henry, G. H. Relative impacts of disturbance and temperature: persistent changes in microenvironment and vegetation in retrogressive thaw slumps. *Glob. Change Biol.* **15**, 1664-1675, doi:https://doi.org/10.1111/j.1365-2486.2009.01917.x (2009).

13 Myers-Smith, I. H. *et al.* Shrub expansion in tundra ecosystems: dynamics, impacts and research priorities. *Environ. Res. Lett.* **6**, doi:https://doi.org/10.1088/1748-9326/6/4/045509 (2011).

14 Stow, D. A. *et al.* Remote sensing of vegetation and land-cover change in Arctic Tundra Ecosystems. *Remote Sens. Environ.* **89**, 281-308, doi:https://doi.org/10.1016/j.rse.2003.10.018 (2004).

15 Bhatt, U. S. *et al.* Recent Declines in Warming and Vegetation Greening Trends over Pan-Arctic Tundra. *Remote Sens.* **5**, 4229-4254, doi:https://doi.org/10.3390/rs5094229 (2013).

16 Berner, L. T. *et al.* Summer warming explains widespread but not uniform greening in the Arctic tundra biome. *Nat. Commun.* **11**, 4621, doi:https://doi.org/10.1038/s41467-020-18479-5 (2020).

17 Sistla, S. A. *et al.* Long-term warming restructures Arctic tundra without changing net soil carbon storage. *Nature* **497**, 615-618, doi:http://dx.doi.org/10.1038/nature12129 (2013).

18 Blok, D. *et al.* Shrub expansion may reduce summer permafrost thaw in Siberian tundra. *Glob. Change Biol.* **16**, 1296-1305, doi:https://doi.org/10.1111/j.1365-2486.2009.02110.x (2010).

19 Loranty, M. M., Goetz, S. J. & Beck, P. S. A. Tundra vegetation effects on pan-Arctic albedo. *Environ. Res. Lett.* **6**, doi:https://doi.org/10.1088/1748-9326/6/2/024014 (2011).

20 Pearson, R. G. *et al.* Shifts in Arctic vegetation and associated feedbacks under climate change. *Nature Climate Change* **3**, 673-677, doi:https://doi.org/10.1038/nclimate1858 (2013).

21 Rocha, A. V. *et al.* The footprint of Alaskan tundra fires during the past half-century: implications for surface properties and radiative forcing. *Environ. Res. Lett.* **7**, 044039, doi:https://doi.org/10.1088/1748-9326/7/4/044039 (2012).

22 Mack, M. C. *et al.* Carbon loss from an unprecedented Arctic tundra wildfire. *Nature* **475**, 489-492, doi:https://doi.org/10.1038/nature10283 (2011).

23 Higuera, P. E., Chipman, M. L., Barnes, J. L., Urban, M. A. & Hu, F. S. Variability of tundra fire regimes in Arctic Alaska: millennial-scale patterns and ecological implications. *Ecol. Appl.* **21**, 3211-3226, doi:https://doi.org/10.1890/11-0387.1 (2011).

24 Higuera, P. E. *et al.* Frequent fires in ancient shrub tundra: implications of paleorecords for arctic environmental change. *PLoS One* **3**, e0001744, doi:https://doi.org/10.1371/journal.pone.0001744 (2008).

25 Hu, F. S. *et al.* Arctic tundra fires: natural variability and responses to climate change. *Frontiers in Ecology and the Environment* **13**, 369-377, doi:https://doi.org/10.1890/150063 (2015).

26 French, N. H. F. *et al.* Fire in arctic tundra of Alaska: past fire activity, future fire potential, and significance for land management and ecology. *Int. J. Wildland Fire* **24**, 1045-1061, doi:https://doi.org/10.1071/WF14167 (2015).

27 Camac, J. S., Williams, R. J., Wahren, C.-H., Hoffmann, A. A. & Vesk, P. A. Climatic warming strengthens a positive feedback between alpine shrubs and fire. *Glob. Change Biol.* **23**, 3249-3258, doi:https://doi.org/10.1111/gcb.13614 (2017).

28 Gaglioti, B. V. *et al.* Tussocks Enduring or Shrubs Greening: Alternate Responses to Changing Fire Regimes in the Noatak River Valley, Alaska. *Journal of Geophysical Research: Biogeosciences* **126**, e2020JG006009, doi:https://doi.org/10.1029/2020JG006009 (2021).

29 Chen, Y., Hu, F. S. & Lara, M. J. Divergent shrub-cover responses driven by climate, wildfire, and permafrost interactions in Arctic tundra ecosystems. *Glob. Change Biol.* **27**, 652-663, doi:https://doi.org/10.1111/gcb.15451 (2021).

30 Fastie, C. L., Lloyd, A. H. & Doak, P. Fire history and postfire forest development in an upland watershed of interior Alaska. *J. Geophys. Res.-Atmos.* **108**, doi:https://doi.org/10.1029/2001jd000570 (2002).

31 Racine, C., Jandt, R., Meyers, C. & Dennis, J. Tundra Fire and Vegetation Change along a Hillslope on the Seward Peninsula, Alaska, U.S.A. *Arctic, Antarctic, and Alpine Research* **36**, 1-10, doi:https://doi.org/10.1657/1523-0430(2004)036[0001:TFAVCA]2.0.CO;2 (2004).

32 Higuera, P. E., Brubaker, L. B., Anderson, P. M., Hu, F. S. & Brown, T. A. Vegetation mediated the impacts of postglacial climate change on fire regimes in the south-central Brooks Range, Alaska. *Ecol. Monogr.* **79**, 201-219, doi:https://doi.org/10.1890/07-2019.1 (2009).

33 Bailey, A. W. & Anderson, M. L. Fire temperatures in grass, shrub and aspen forest communities of Central Alberta. *Journal of Range Management Archives* **33**, 37-40, doi:https://doi.org/10.2307/3898225 (1980).

34 Blok, D. *et al.* The response of Arctic vegetation to the summer climate: relation between shrub cover, NDVI, surface albedo and temperature. *Environ. Res. Lett.* **6**, 035502, doi:https://doi.org/10.1088/1748-9326/6/3/035502 (2011).

35 Tape, K. E. N., Sturm, M. & Racine, C. The evidence for shrub expansion in Northern Alaska and the Pan-Arctic. *Glob. Change Biol.* **12**, 686-702, doi:http://dx.doi.org/10.1111/j.1365-2486.2006.01128.x (2006).

36 Forbes, B. C., Fauria, M. M. & Zetterberg, P. Russian Arctic warming and 'greening' are closely tracked by tundra shrub willows. *Glob. Change Biol.* **16**, 1542-1554, doi:https://doi.org/10.1111/j.1365-2486.2009.02047.x (2010).

37 Berner, L. T., Jantz, P., Tape, K. D. & Goetz, S. J. Tundra plant above-ground biomass and shrub dominance mapped across the North Slope of Alaska. *Environ. Res. Lett.* **13**, 035002, doi:https://doi.org/10.1088/1748-9326/aaaa9a (2018).

38 Boelman, N. T. *et al.* Response of NDVI, biomass, and ecosystem gas exchange to long-term warming and fertilization in wet sedge tundra. *Oecologia* **135**, 414-421, doi:https://doi.org/10.1007/s00442-003-1198-3 (2003).

39 Walker, D. A. *et al.* Phytomass, LAI, and NDVI in northern Alaska: Relationships to summer warmth, soil pH, plant functional types, and extrapolation to the circumpolar Arctic. *Journal of Geophysical Research: Atmospheres* **108**, doi:https://doi.org/10.1029/2001JD000986 (2003).

40 Raynolds, M. K., Walker, D. A. & Maier, H. A. NDVI patterns and phytomass distribution in the circumpolar Arctic. *Remote Sens. Environ.* **102**, 271-281, doi:https://doi.org/10.1016/j.rse.2006.02.016 (2006).

41 Johansen, B. & Tømmervik, H. The relationship between phytomass, NDVI and vegetation communities on Svalbard. *Int. J. Appl. Earth Obs. Geoinf.* **27**, 20-30, doi:https://doi.org/10.1016/j.jag.2013.07.001 (2014).

42 Cunliffe, A. M., J Assmann, J., N Daskalova, G., Kerby, J. T. & Myers-Smith, I. H. Aboveground biomass corresponds strongly with drone-derived canopy height but weakly with greenness (NDVI) in a shrub tundra landscape. *Environ. Res. Lett.* **15**, 125004, doi:https://doi.org/10.1088/1748-9326/aba470 (2020).

43 Bret-Harte, M. S. *et al.* The response of Arctic vegetation and soils following an unusually severe tundra fire. *Philosophical Transactions of the Royal Society B: Biological Sciences* **368**, doi:http://dx.doi.org/10.1098/rstb.2012.0490 (2013).

44 Wein, R. W. & Bliss, L. C. Changes in Arctic Eriophorum Tussock Communities Following Fire. *Ecology* **54**, 845-852, doi:https://doi.org/10.2307/1935679 (1973).

45 Racine, C. H., Johnson, L. A. & Viereck, L. A. Patterns of Vegetation Recovery after Tundra Fires in Northwestern Alaska, U.S.A. *Arctic and Alpine Research* **19**, 461-469, doi:https://doi.org/10.1080/00040851.1987.12002628 (1987).

46 Loboda, T. V., Jenkins, L. K., Chen, D., He, J. & Baer, A. (ORNL Distributed Active Archive Center, Oak Ridge, Tennessee, USA, 2022).

47 Macander, M. J., Frost, G. V., Nelson, P. R. & Swingley, C. S. (ORNL Distributed Active Archive Center, 2021).

48 Frost, G. V., Loehman, R. A., Nelson, P. R. & Paradis, D. P. (ORNL Distributed Active Archive Center, 2020).

49 Walker, D. A. *et al.* The Circumpolar Arctic vegetation map. *J. Veg. Sci.* **16**, 267-282, doi:https://doi.org/10.1111/j.1654-1103.2005.tb02365.x (2005).

50 Muller, S., Walker, D. A. & Jorgenson, M. T. (ORNL Distributed Active Archive Center, 2018).

51 Raynolds, M. K. *et al.* A raster version of the Circumpolar Arctic Vegetation Map (CAVM). *Remote Sens. Environ.* **232**, 111297, doi:https://doi.org/10.1016/j.rse.2019.111297 (2019).

52 Hu, F. S. *et al.* Tundra burning in Alaska: Linkages to climatic change and sea ice retreat. *J. Geophys. Res.-Biogeosci.* **115**, doi:https://doi.org/10.1029/2009jg001270 (2010).

53 Chipman, M. L. *et al.* Spatiotemporal patterns of tundra fires: late-Quaternary charcoal records from Alaska. *Biogeosciences* **12**, 4017-4027, doi:https://doi.org/10.5194/bg-12-4017-2015 (2015).

54 Heijmans, M. M. P. D. *et al.* Tundra vegetation change and impacts on permafrost. *Nature Reviews Earth & Environment* **3**, 68-84, doi:https://doi.org/10.1038/s43017-021-00233-0 (2022).

55 Rupp, T. S., Starfield, A. M. & Chapin, F. S. A frame-based spatially explicit model of subarctic vegetation response to climatic change: comparison with a point model. *Landsc. Ecol.* **15**, 383-400, doi:https://doi.org/10.1023/A:1008168418778 (2000).

56 Hollingsworth, T. N., Breen, A. L., Hewitt, R. E. & Mack, M. C. Does fire always accelerate shrub expansion in Arctic tundra? Examining a novel grass-dominated successional trajectory on the Seward Peninsula. *Arctic, Antarctic, and Alpine Research* **53**, 93-109, doi:https://doi.org/10.1080/15230430.2021.1899562 (2021).

57 Lara, M. J., Nitze, I., Grosse, G., Martin, P. & McGuire, A. D. Reduced arctic tundra productivity linked with landform and climate change interactions. *Scientific Reports* **8**, 2345, doi:https://doi.org/10.1038/s41598-018-20692-8 (2018).

58 Loranty, M. M. *et al.* Spatial variation in vegetation productivity trends, fire disturbance, and soil carbon across arctic-boreal permafrost ecosystems. *Environ. Res. Lett.* **11**, 095008, doi:https://doi.org/10.1088/1748-9326/11/9/095008 (2016).

59 Bjorkman, A. D. *et al.* Plant functional trait change across a warming tundra biome. *Nature* **562**, 57-62, doi:https://doi.org/10.1038/s41586-018-0563-7 (2018).

60 Myers-Smith, I. H. *et al.* Climate sensitivity of shrub growth across the tundra biome. *Nature Clim. Change* **5**, 887-891, doi:https://doi.org/10.1038/nclimate2697 (2015).

61 Martin, A. C., Jeffers, E., Petrokofsky, G., Myers-Smith, I. & Macias-Fauria, M. Shrub growth and expansion in the Arctic tundra: an assessment of controlling factors using an evidence-based approach. *Environ. Res. Lett.*, doi:https://doi.org/10.1088/1748-9326/aa7989 (2017).

62 Ackerman, D., Griffin, D., Hobbie, S. E. & Finlay, J. C. Arctic shrub growth trajectories differ across soil moisture levels. *Glob. Change Biol.* **23**, 4294-4302, doi:https://doi.org/10.1111/gcb.13677 (2017).

63 Rocha, A. V., Blakely, B., Jiang, Y., Wright, K. S. & Curasi, S. R. Is arctic greening consistent with the ecology of tundra? Lessons from an ecologically informed mass balance model. *Environ. Res. Lett.* **13**, 125007, doi:http://dx.doi.org/10.1088/1748-9326/aaeb50 (2018).

64 Masrur, A., Petrov, A. N. & DeGroote, J. Circumpolar spatio-temporal patterns and contributing climatic factors of wildfire activity in the Arctic tundra from 2001–2015. *Environ. Res. Lett.* **13**, 014019, doi:https://doi.org/10.1088/1748-9326/aa9a76 (2018).

65 Chen, D., Shevade, V., Baer, A. E. & Loboda, T. V. Missing burns in the high northern latitudes: The case for regionally focused burned area products. *Remote Sens.* **13**, 4145, doi:https://doi.org/10.3390/rs13204145 (2021).

66 Jones, B. M. *et al.* Identification of unrecognized tundra fire events on the north slope of Alaska. *J. Geophys. Res.-Biogeosci.* **118**, 1334-1344, doi:https://doi.org/10.1002/jgrg.20113 (2013).

67 Frost, G. V. *et al.* Multi-decadal patterns of vegetation succession after tundra fire on the Yukon-Kuskokwim Delta, Alaska. *Environ. Res. Lett.* **15**, 025003, doi:https://doi.org/10.1088/1748-9326/ab5f49 (2020).

68 Bintanja, R. & Selten, F. M. Future increases in Arctic precipitation linked to local evaporation and sea-ice retreat. *Nature* **509**, 479-482, doi:https://doi.org/10.1038/nature13259 (2014).

69 Bintanja, R. & Andry, O. Towards a rain-dominated Arctic. *Nature Climate Change* **7**, 263-267, doi:https://doi.org/10.1038/nclimate3240 (2017).

70 Vanha-Majamaa, I. *et al.* Rehabilitating boreal forest structure and species composition in Finland through logging, dead wood creation and fire: The EVO experiment. *Forest Ecology and Management* **250**, 77-88, doi:https://doi.org/10.1016/j.foreco.2007.03.012 (2007).

71 Hinzman, L. D., Fukuda, M., Sandberg, D. V., Chapin III, F. S. & Dash, D. FROSTFIRE: An experimental approach to predicting the climate feedbacks from the changing boreal fire regime. *Journal of Geophysical Research: Atmospheres* **108**, FFR 9-1-FFR 9-6, doi:https://doi.org/10.1029/2001jd000415 (2003).

72 Hély, C., Fortin, C. M.-J., Anderson, K. R. & Bergeron, Y. Landscape composition influences local pattern of fire size in the eastern Canadian boreal forest: role of weather and landscape mosaic on fire size distribution in mixedwood boreal forest using the Prescribed Fire Analysis System. *Int. J. Wildland Fire* **19**, 1099-1109, doi:https://doi.org/10.1071/WF09112 (2010).

73 Loboda, T. V., French, N. H. F., Hight-Harf, C., Jenkins, L. & Miller, M. E. Mapping fire extent and burn severity in Alaskan tussock tundra: An analysis of the spectral response of tundra vegetation to wildland fire. *Remote Sens. Environ.* **134**, 194-209, doi:http://dx.doi.org/10.1016/j.rse.2013.03.003 (2013).

74 Smith, W. B. & Brand, G. J. Allometric biomass equations for 98 species of herbs, shrubs, and small trees. *Research Note NC-299. St. Paul, MN: US Dept. of Agriculture, Forest Service, North Central Forest Experiment Station* **299** (1983).

75 Masek, J. G. *et al.* A Landsat surface reflectance dataset for North America, 1990-2000. *Geoscience and Remote Sensing Letters, IEEE* **3**, 68-72, doi:http://dx.doi.org/10.1109/LGRS.2005.857030 (2006).

76 Vermote, E., Justice, C., Claverie, M. & Franch, B. Preliminary analysis of the performance of the Landsat 8/OLI land surface reflectance product. *Remote Sens. Environ.* **185**, 46-56, doi:https://doi.org/10.1016/j.rse.2016.04.008 (2016).

77 Eidenshink, J. C. *et al.* A project for monitoring trends in burn severity. *Fire Ecology* **3**, 3-21, doi:https://doi.org/10.4996/fireecology.0301003 (2007).

78 Pekel, J.-F., Cottam, A., Gorelick, N. & Belward, A. S. High-resolution mapping of global surface water and its long-term changes. *Nature* **540**, 418-422, doi:https://doi.org/10.1038/nature20584 (2016).

79 Myers-Smith, I. H. *et al.* Complexity revealed in the greening of the Arctic. *Nature Climate Change* **10**, 106-117, doi:https://doi.org/10.1038/s41558-019-0688-1 (2020).